Article

Analysis of Adsorption and Decomposition of Odour and Tar Components in Tobacco Smoke on Non-Woven Fabric-Supported Photocatalysts

Tsuyoshi Ochiai [1,2,*] , **Daisuke Aoki [1]** , **Hidenori Saito [1]** , **Yasuhisa Akutsu [1]** and **Morio Nagata [3]**

[1] Kawasaki Technical Support Department, Local Independent Administrative Agency Kanagawa Institute of Industrial Science and TEChnology (KISTEC), Ground Floor East Wing, Innovation Center Building, KSP, 3-2-1 Sakado, Takatsu-ku, Kawasaki, Kanagawa 213-0012, Japan; d-aoki@kistec.jp (D.A.); hidenori.saito@kistec.jp (H.S.); akutsu@kistec.jp (Y.A.)

[2] Photocatalysis International Research Center, Tokyo University of Science, 2641 Yamazaki, Noda, Chiba 278-8510, Japan

[3] Department of Industrial Chemistry, Graduate School of Engineering, Tokyo University of Science, 12-1 Ichigayafunagawara-cho, Shinjuku-ku, Tokyo 162-0826, Japan; nagata@ci.tus.ac.jp

* Correspondence: ochiai.tsuyoshi@gmail.com; Tel.: +81-44-819-2105

check for updates

Abstract: The release of substantial amounts of toxicologically significant, irritant, and malodourous compounds during the complete combustion of tobacco can generate an unpleasant environment, especially indoors. Herein, we developed non-woven fabric-supported UV- and visible-light-responsive photocatalysts capable of adsorbing and decomposing the odour and tar components of tobacco smoke under irradiation with UV or visible light. The processes of odour component adsorption and subsequent decomposition under irradiation were evaluated in terms of colour changes in the catalytic system and by gas chromatography–mass spectrometry. By considering three different photocatalysts, namely TiO_2, Fe(III)-grafted TiO_2, and Cu(II)-grafted WO_3, we assessed the magnitude of odour and tar component adsorption on the fabric fibres, as well as the decomposition of these species after specific visible light or UV irradiation periods. Considering the expansion of our technology for practical applications, the best results among the three tested materials were obtained for non-woven fabric-supported Fe/TiO_2. We believe that our technology can be implemented in the design of interior decoration materials for creating a comfortable environment.

1. Introduction

In recent years, third-hand smoke has been identified as a new, hazardous, and unpleasant consequence of cigarette smoking [1]. It comprises all the chemical residues resulting from smoking tobacco, which soak into clothing, upholstery, walls, furniture, hair, and other objects even after the cigarette has been put out. These deposits remain attached to the host material for months, and are hard to eliminate using common ventilation systems, hence causing serious health consequences not only for smokers but for whoever enters a contaminated environment [2]. In addition, a recent study revealed that hazardous airborne emissions can be generated not only from burning cigarettes but also from extinguished cigarette butts [3]. In this regard, some companies in Japan are encouraging visitors not only to avoid smoking in their offices or locations, but even before getting there.

Photocatalysts have demonstrated strong oxidation abilities in redox systems since they were first reported in the 1970s [4]; as most pollutants in the atmosphere can be removed by several kinds

of active oxidative species, photocatalysts are widely used in air purification systems [5]. In recent years, multiple practical air purifiers have been developed, based on photocatalysis, which can decompose the main tobacco smoke contaminants [6–8]. However, although numerous practical air purifiers for tobacco smoke have developed, very few studies have focused on the fundamental understanding, and report standard methods of analysis, of the adsorption and decomposition of odour and tar constituents in tobacco smoke trapped on clothes or other materials. On the other hand, tailored semiconductor heterostructures come into prominence as the forefront of photocatalyst development [9,10]. In particular, composites prepared by the grafting of metal species on a TiO_2 surface can absorb visible light because of interfacial charge transfer (IFCT) from TiO_2 to metal ions [11,12]. This visible-light activity is important in practical applications such as the fabrication of interior materials, clothes, and fabrics.

In this study, we developed a non-woven fabric-supported, UV- and visible-light-responsive photocatalyst, fashioned to adsorb and decompose the hazardous components in tobacco smoke under UV or visible light irradiation. Tobacco smoke is comprised of airborne particulates and gases. The particulates may be composed of drops of condensed heavier hydrocarbons called 'tar', which exhibit a yellow to brown colour. The gases are mainly volatile organic compounds (VOCs), which have a pungent odour and are harmful to inhale. Therefore, by evaluating the changes in colour of the system, and by gas chromatography–mass spectrometry (GC-MS) analysis, we could establish the magnitude of adsorption of the odour and tar components and their subsequent decomposition under light irradiation, and quantify each process. Our material might be engineered in the future as a constituent of textile and upholstery materials and applied in interior furnishing to avoid the persistence of third-hand smoke, and create comfortable and pleasant indoor environments.

2. Results

2.1. Preparation of the Non-Woven Fabric-Supported Photocatalysts

Figure 1a shows the scanning electron microscopy (SEM) image of pristine non-woven fabric, whose fibres are made of a thermoplastic resin; the fibres have diameters of 10–20 μm with a smooth surface. On the other hand, the SEM images of the fabric after modification with the host UV-responsive photocatalyst, TiO_2 P 25, are shown in Figure 1b, evidencing that the TiO_2 films are made up of sub-micron particles. These fabrics show a similar morphology with fabrics that we previously prepared and analysed by SEM and X-ray diffraction (XRD) [13]. The SEM images of the fabrics embedded with Fe/TiO_2 and Cu/WO_3, the visible-light-responsive photocatalysts, are shown in Figure 1c,d, respectively. These figures indicate that photocatalyst particles were successfully immobilised on the surface of the fabric. Due to the different loading levels achievable with the different photocatalysts, the morphologies of the fibres of the three fabric samples are different, even though the adhered particles have the same size and shape: the loading levels for Fe/TiO_2 and Cu/WO_3 on the fabric surface could be as high as 18.6 and 89.4 g/m^2, respectively, while TiO_2 loading could only reach 6.0 g/m^2. Therefore, the former fabrics show high photocatalyst density.
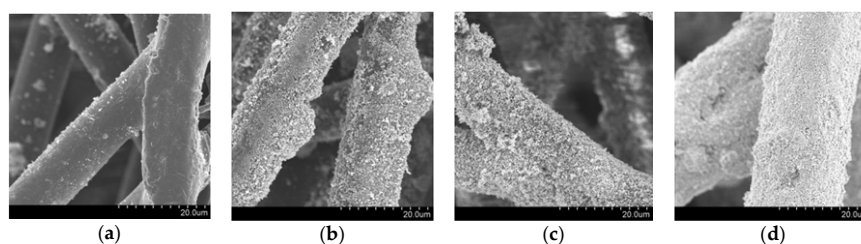

| (a) | (b) | (c) | (d) |

Figure 1. Scanning electron microscopy (SEM) images of (**a**) non-woven fabric fibres before adding the host photocatalyst; (**b**) non-woven fabric with UV-responsible photocatalyst (TiO_2 P 25); (**c**) non-woven fabric with visible-light-responsive photocatalyst (Fe/TiO_2); (**d**) non-woven fabric with visible-light-responsive photocatalyst (Cu/WO_3).

2.2. Adsorption and Decomposition of the Odour and Tar Components on the TiO$_2$-Embedded Fabrics

Figure 2 shows the normalised GC-MS chromatograms of the solid phase-extracted odour components from non-woven fabric samples with and without TiO$_2$. Many peaks attributable to VOCs were observed in the chromatogram of the fabric with TiO$_2$ after tobacco smoke adsorption, and before UV treatment (= 0 h of UV irradiation, hereafter defined as "0 h"), which had decreased after 24 h of irradiation. The total VOC (TVOC) concentrations were calculated for all the peaks located between the elution times of n-hexane (16 min) and n-hexadecane (53 min) according to a reported method; they were then calibrated and converted to toluene peak equivalents (located at 30 min of elution time) [8,14]. For the TiO$_2$-embedded fabrics, the TVOC concentrations at 0 and 24 h were 0.91 and 0.25 µg/m^3, respectively (corresponding to 73% removal ratio of TVOCs, Figure 2a). On the other hand, although the non-woven fabric without TiO$_2$ shows almost the same TVOC concentration as its modified counterpart at 0 h (0.93 µg/m^3), the VOC peaks remained almost unchanged after 24 h of irradiation (Figure 2b). These data indicate that the VOCs could be degraded by the photocatalyst.
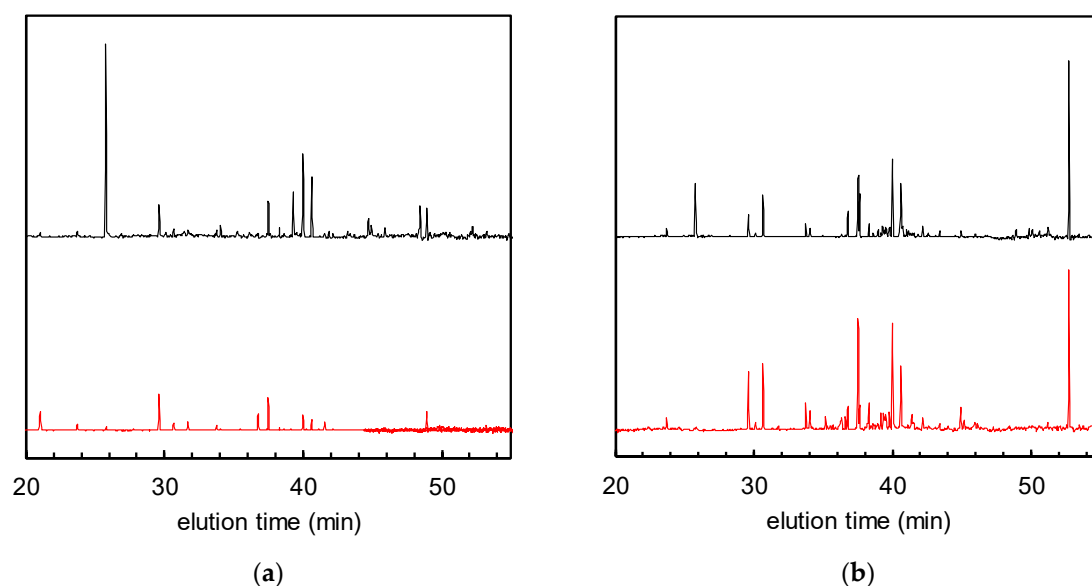

Figure 2. Gas chromatograms of solid phase-extracted odour components after tobacco smoke adsorption (= 0 h of UV irradiation, black) and after 24 h of UV irradiation (red). (**a**) Non-woven fabric with TiO$_2$; (**b**) non-woven fabric without TiO$_2$.

We could observe that, after tobacco smoke adsorption, the non-woven fabric with TiO$_2$ dramatically changed colour, due to the uptake of the tar components (Figure 3a). The colour difference (evaluated with the ΔE^*_{ab} scale) of the fabric after tobacco smoke adsorption at 0 h compared to the fabric before tobacco smoke adsorption was 5.4. After 24 h of UV irradiation, the ΔE^*_{ab} value, relative to the colour of the fabric before tobacco smoke adsorption, became 0.6; these colour differences can be easily perceived by the naked eye, with the 24-h sample looking almost white (Figure 3a, right end). This indicates that the adsorbed tar components had almost entirely decomposed after UV irradiation in the presence of the photocatalyst [6]. On the other hand, the colour of the non-woven fabric without TiO$_2$ did not change significantly after tobacco smoke adsorption (ΔE^*_{ab} = 0.7, Figure 3b).

Figure 4 summarises the time course of the TVOC concentration (red) and the colour difference (blue) of the fabrics with and without TiO$_2$. Due to an increase in active surface area after TiO$_2$ absorption, a tangible difference was observed in pollutants uptake. Regardless of the pollutants' composition, after 24 h of UV irradiation, the amounts of both tar and odour could be almost totally reduced by photocatalysis.

Figure 3. Photographs of the non-woven fabrics before tobacco smoke adsorption, after tobacco smoke adsorption (0 h), and after 24 h of UV irradiation. (**a**) Non-woven fabric with TiO_2; (**b**) non-woven fabric without TiO_2.
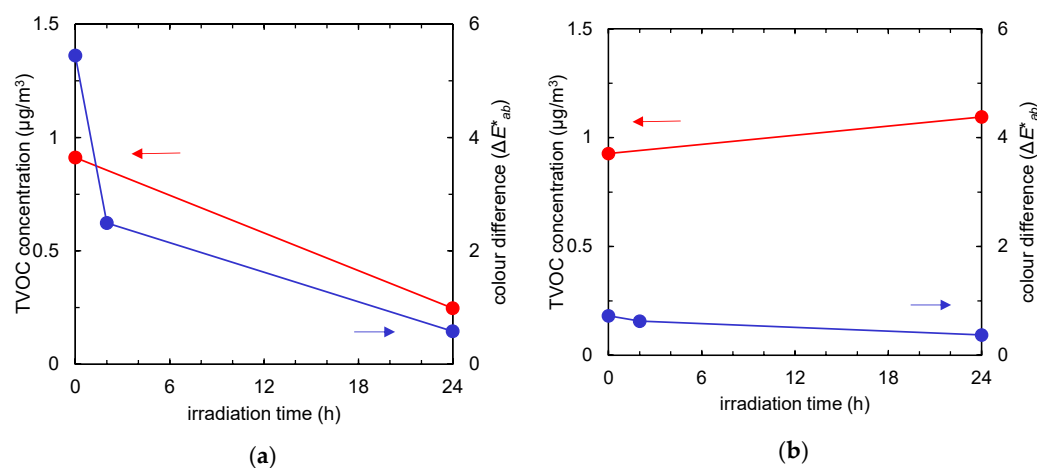

Figure 4. Time course of total volatile organic compound (TVOC) concentration (red) and colour difference (the ΔE^*_{ab} value compared to the colour of the fabric before tobacco smoke adsorption, represented in blue) of the fabrics after tobacco smoke adsorption vs. UV irradiation time. (**a**) Non-woven fabric with TiO_2; (**b**) non-woven fabric without TiO_2.

2.3. Adsorption and Decomposition of Odour and Tar Components on the Fabrics Modified with Visible-Light-Activated Photocatalysts

Figure 5 shows the normalised GC-MS chromatograms of the solid-phase-extracted odour components from the non-woven fabric samples with and without Fe/TiO_2. Similar to the previous case, the VOC peaks decreased after 24 h of visible light irradiation, with a removal ratio of TVOC of 55% (Figure 5a). On the other hand, the VOC peaks remained almost unchanged in the chromatogram of the pristine non-woven fabric after 24 h of visible light irradiation (Figure 5b). These data indicate that the VOCs could also be removed by visible-light-induced photocatalysis.

Figures 6 and 7 show the colour changes of a Fe/TiO_2-embedded fabric sample subject to visible light irradiation, and the time courses of TVOC concentrations and colour differences, respectively. The colour difference of the fabric after 0 h of irradiation compared to the initial colour was 10.4 (Figure 6, left end). After 24 h of visible light irradiation, the ΔE^*_{ab} value decreased to 3.6 (Figure 6, right end; Figure 7a, blue line). This indicates that the tar constituents were also decomposed by visible-light-induced photocatalysis. On the other hand, the pristine non-woven fabric shows a small colour change after 24 h of visible light irradiation (ΔE^*_{ab} dropped from 2.7 to 1.2, Figure 7b, blue line).
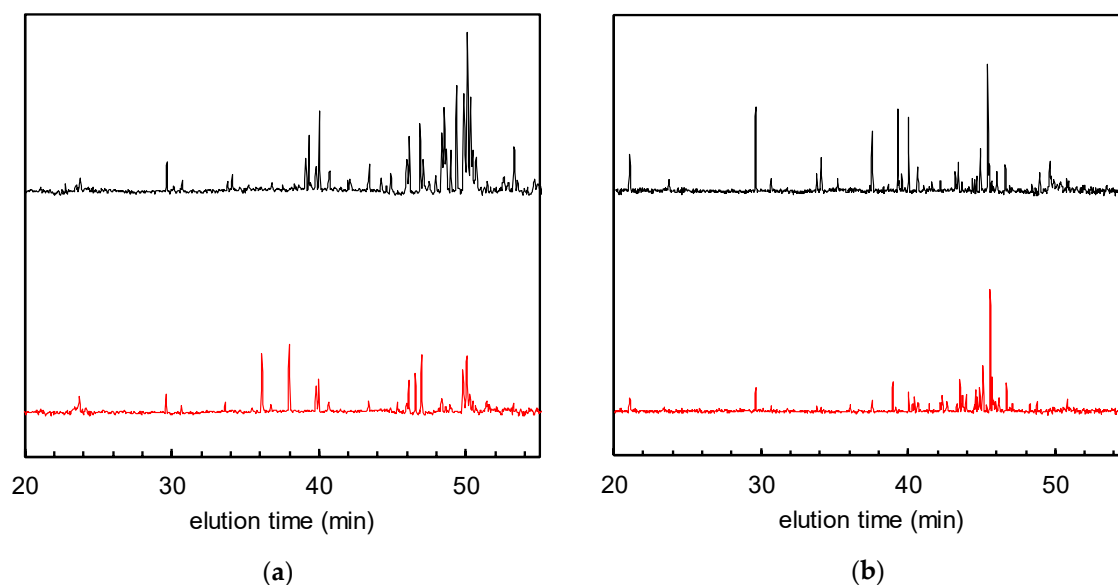
Figure 5. Gas chromatograms of solid-phase-extracted odour components after tobacco smoke adsorption (= 0 h of visible light irradiation) (black) and 24 h (red) of visible light irradiation. (**a**) Non-woven fabric with Fe/TiO$_2$; (**b**) non-woven fabric without Fe/TiO$_2$.
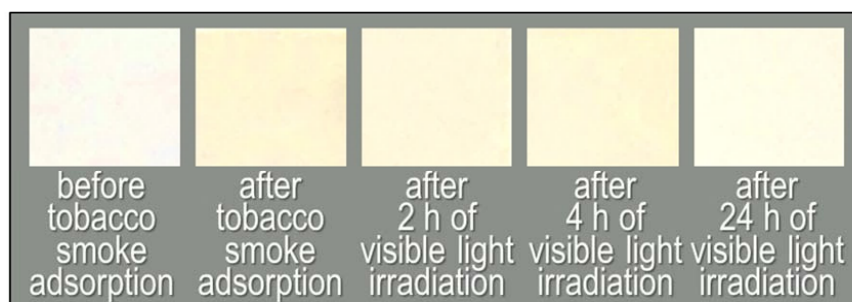

Figure 6. Photographs of the non-woven fabric with Fe/TiO$_2$ before tobacco smoke adsorption, after tobacco smoke adsorption (0 h) and after 2, 4, and 24 h of visible light irradiation.
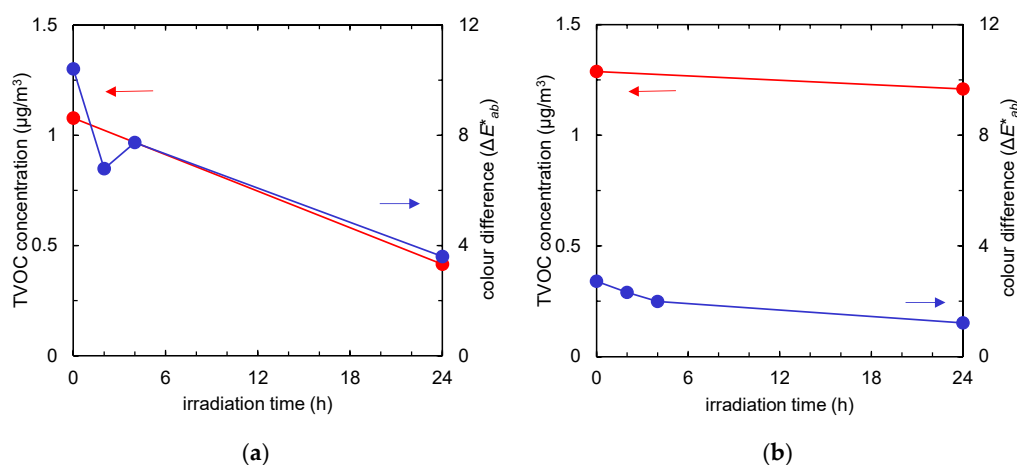

Figure 7. Time course of total volatile organic compound (TVOC) concentration (red) and the colour difference (the ΔE^*_{ab} value compared to the colour of the fabric before tobacco smoke adsorption, shown by the blue line) of the fabrics after tobacco smoke adsorption vs. visible light irradiation time. (**a**) Non-woven fabric with Fe/TiO$_2$; (**b**) non-woven fabric without Fe/TiO$_2$.

Another type of visible-light-activated photocatalyst, Cu/WO_3, showed different results, and Figures 8 and 9 report the behaviour of the non-woven fabric samples embedded with this catalyst. Although the normalised GC-MS chromatograms of the solid-phase-extracted odour components (Figure 8a) and the time course graphs of TVOC concentration (Figure 8b, red line) indicate that the odour components were decomposed, the colour did not revert to white after 24 h of irradiation (Figure 8b, blue line); instead, the colour of the fabric changed from yellow to dark yellow (Figure 9).
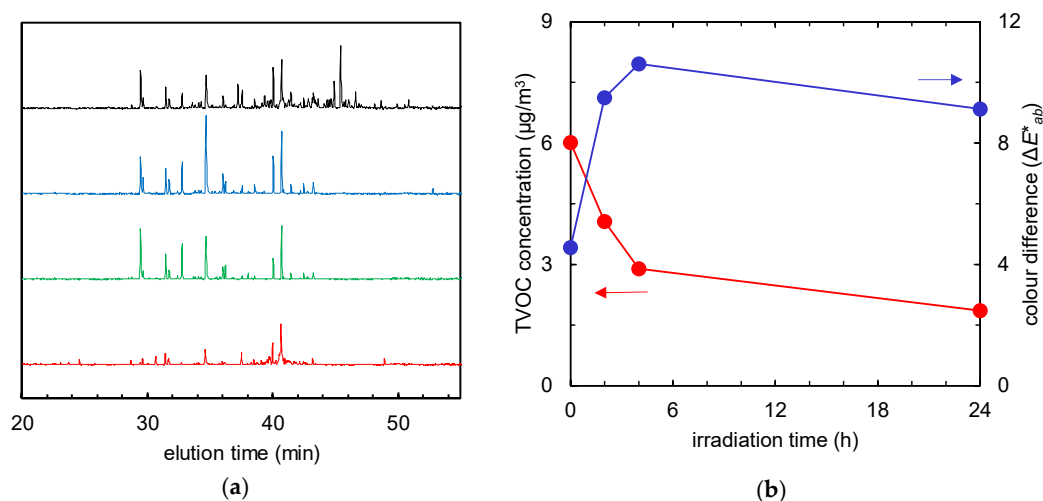

Figure 8. (**a**) Gas chromatographs of solid-phase-extracted odour components at 0 h (black), and after 2 (blue), 4 (green), and 24 h (red) of visible light irradiation. (**b**) Time course of total volatile organic compound (TVOC) concentration (red) and the colour difference (the ΔE^*_{ab} value compared to the colour of the fabric before tobacco smoke adsorption, blue) of the fabrics with Cu/WO_3 after tobacco smoke adsorption vs. visible light irradiation time.
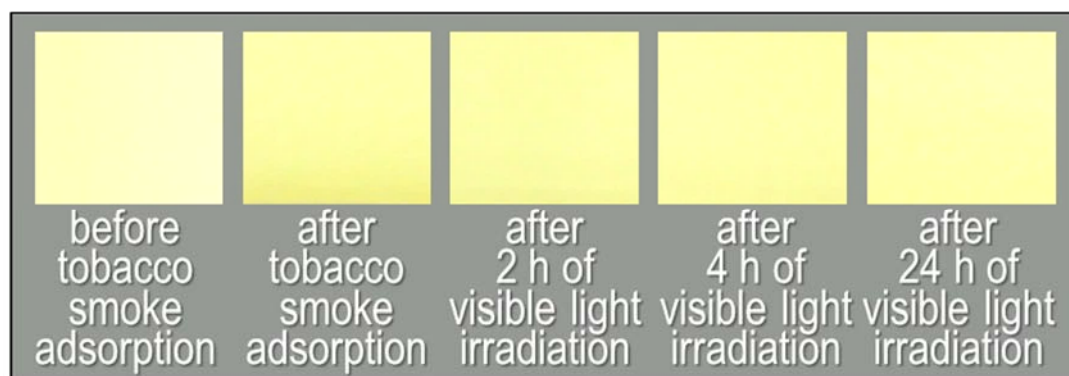

Figure 9. Photographs of the non-woven fabric with Cu/WO_3 before tobacco smoke adsorption, after tobacco smoke adsorption (0 h), and after 2, 4, and 24 h of visible light irradiation.

3. Discussion

As can be seen from Figure 1, the three photocatalysts were successfully immobilised on the surface of the fibres, but could be loaded in different quantities. We speculate that these substantial differences in loading level may be caused by a high affinity between the visible-light-responsive photocatalysts and the fabric material. The conditions used to load the catalysts onto the non-woven fabrics might also play a role the heating and blowing steps, in which the catalysts were heated to above the melting point of the plastic and blown onto the thermoplastic fibre surface. Moreover, we might conclude that the higher the loading, the higher the photocatalytic activity. However, the different catalysts function through different mechanisms, and the overall pollutant uptake and conversion might be imputable to multiple factors.

For the odour constituents, according to GC-MS analysis, there is almost no difference in adsorption between the samples with and without TiO$_2$ (Figure 2). On the other hand, for the tar components, there are significant differences (Figure 3). The fabric used in this study is non-porous, with a small surface area, and hence, a low adsorption ability. However, the embedding of the TiO$_2$ particles increased the surface area of the fabric and caused a tangible difference in its adsorption ability. These adsorption properties especially affected the tar contents and resulted in a significant difference in colour between the samples with and without TiO$_2$ (Figure 3). These results indicate that the adsorption kinetics of the odour constituents is different from that of the tar components. Several researchers have reported the efficiency of the adsorption of oils onto TiO$_2$-embedded materials [15,16]; this affinity may cause the observed adsorption behaviour in the case of tar, which is mainly constituted of a mixture of hydrocarbons. Regardless of the uptake differences, odour and tar constituents could be successfully degraded by the strong oxidation ability of TiO$_2$ under UV irradiation [5].

Furthermore, Figures 5, 7 and 8 show that the VOCs could be removed by visible-light-induced photocatalysis.

Fe/TiO$_2$ is obtained by grafting Fe(III) species with an amorphous FeO(OH)-like structure on a rutile TiO$_2$ surface [11]. This system can absorb visible light with $\lambda \geq 400$ nm, attributable to IFCT from TiO$_2$ to the iron ions. In this mechanism, the excited electrons reduce Fe(III) to Fe(II) ions, which have the capacity to reduce oxygen, while photo generated holes remain in the valence band of TiO$_2$ and oxidise organic compounds, such as the constituents of cigarette smoke odour, and tar. The Fe/TiO$_2$-embedded fibres showed similar odour and tar components removal behaviour to the TiO$_2$-embedded fibres.

For the third photocatalyst, Cu/WO$_3$, although the normalised GC-MS chromatograms of the solid-phase-extracted odour components (Figure 8a) and the time-course graphs of TVOC concentration (Figure 8b, red line) indicate that the odour components were decomposed, reversion to the initial colour ($\Delta E^*_{ab} = 0$) did not occur after 24-h irradiation (Figure 8b, blue line); instead, the colour of the fabric changed from yellow to dark yellow (Figure 9). When Cu(II) is grafted on the surface of WO$_3$ powder, the same photo-induced IFCT effect occurs from WO$_3$ to Cu(II) ions, as happens for Fe(III) ions in Fe/TiO$_2$. In this system, a catalytic multi-electron oxygen reduction by the Cu(I) ions, caused by Cu(II) reduction, and the strong oxidation power of the holes produced in the valence band of WO$_3$, generate multiple effects: Cu(II) d–d transitions (700–800 nm) [17], a WO$_3$ interbank transition (~460 nm) [12,18], and the absorption due to IFCT from the WO$_3$ to Cu(II) (in the case of IFCT from TiO$_2$ to Cu(II) in Cu(II)/TiO$_2$: ~460 nm [12]; in the case of IFCT from TiO$_2$ to Cu$_x$O clusters in Cu$_x$O/TiO$_2$: 400–500 nm (where 'Cu$_x$O' defines clusters with different Cu contents) [19]) all interplay to generate a complex emission profile. However, the absorption due to IFCT from WO$_3$ to Cu(II) is masked by the interbank transition [12]. The colour change of the Cu/WO$_3$ fabric may be caused by the intervention and interference of the decomposed products with these absorption mechanisms. In addition, the diverse dye molecules in tar adsorbed on the photocatalyst surface may cause self-photosensitisation and be simultaneously decomposed [20]. Given the broad diversity of dye molecule types, this effect is hard to quantify by simple spectrophotometric methods, which highlights the need for novel methods of quantitative dye molecule analysis for accurate estimation.

Table 1 compares the photocatalyst systems used for the removal of tobacco smoke components. Although very few studies have focused on the fundamental understanding of the adsorption and decomposition of odour and tar constituents of tobacco smoke trapped on clothes or other materials, our work achieved relatively high removal ratios of these components, as exemplified by the TVOC decomposition ratio under irradiation with both UV and visible light.

In summary, we aimed to achieve the decomposition of adsorbed harmful compounds by photocatalysis, to develop a smart material immune to third-hand smoke. The visible-light activity is especially important in practical applications, such as in the fabrication of interior materials, clothes, and fabrics. However, to increase the visible-light activity, we noticed that our material is subject to a negative colour change. Moreover, this staining was attributed to the presence of decomposed

harmful products. Although we could assess that the odour components can be totally decomposed, the permanence of tar residues is definitely an obstacle to practical applications. From this viewpoint, among the three materials tested, the non-woven fabrics with Fe/TiO_2 are definitely the better option when considering the expansion of our technology for practical applications, specifically the use of our modified fabric as indoor upholstery materials.

Table 1. Comparison of photocatalyst systems used for the removal of tobacco smoke components.

Material	Target	Adsorption and Decomposition Behaviour	Reference
UV-responsive photocatalysts			
Non-woven fabrics made of a thermoplastic resin modified with TiO_2	5.5 µg of TVOC adsorbed per 1 m^2 of the material; adsorbed tar components	Adsorbed TVOC and decomposition ratio under 1 mW cm^{-2} of UV-A were 1.0 and ∞ times those of the unmodified fabric, respectively;[1] adsorbed tar components and decomposition ratio under 1 mW cm^{-2} of UV-A were 7.5 and 1.8 times those of the unmodified fabric, respectively	This work
Ti mesh modified with TiO_2	410 µg of nicotine vapour and 50 µg of 3-ethenylpyridine vapour in 1 m^3 chamber; adsorbed tar components	Nicotine and 3-ethenylpyridine removal ratios obtained for 7 pieces of the mesh (279 mm × 215 mm each) under 0.7 mW cm^{-2} of UV-C were 1.0 and 2.7 times those obtained in the dark, respectively;[2] adsorbed tar components were almost totally decomposed by 32-h illumination with 1.2 mW cm^{-2} of UV-A[3]	[6]
Visible-light-responsive photocatalysts			
Non-woven fabrics made of a thermoplastic resin modified with Fe/TiO_2	7.8 µg of TVOC adsorbed per 1 m^2 of the material; adsorbed tar components	Adsorbed TVOC and decomposition ratio under 10,000 lux of visible light were 1.0 and 9.1 times those of the unmodified fabric, respectively; adsorbed tar components and decomposition ratio under 10,000 lux of visible light were 3.8 and 1.2 times those of the unmodified fabric, respectively	This work
Glass plate coated with visible-light-driven photocatalyst, ILUMIO®	Odour concentration level of 74 in 5-L gas bag	Decomposition ratio under 1000 lux of visible light for 50 cm^2 of the plate was 4.0 times that of the uncoated plate	[21]
polypropylene fibres modified with TiO_2/Ag (modified ethanol dispersion fibre after friction)	151.4 µg of nicotine adsorbed per 1 g of the material	Adsorbed nicotine concentration and decomposition rate constant upon irradiation with solar light passing through a glass window were 5.2 and 1.8 times those of the unmodified fibre, respectively	[22]

[1] The decomposition ratio of the unmodified fabric could not be calculated. [2] Adsorption and decomposition were observed simultaneously. [3] Control experiments were not carried out.

4. Materials and Methods

TiO_2 P 25 (Evonik Industries) was selected as the UV-responsive photocatalyst. Fe(III)-grafted rutile TiO_2 (Fe/TiO_2) [11] and Cu(II)-grafted WO_3 (Cu/WO_3) [12], prepared following the reported procedures, were selected as the visible-light-responsive photocatalysts. Non-woven fabrics, made of a thermoplastic resin (Japan Vilene Co., Ltd., Tokyo, Japan), were used as the support for the photocatalysts. The different catalyst powders were heated above the thermoplastic resin's melting point, and were loaded onto the resin by blowing onto the thermoplastic resin's surface. The surface of the fabrics was observed by scanning electron microscopy (SEM; S-4800, Hitachi High-Technologies Corporation, Tokyo, Japan). The colour differences of the fabrics were measured using a colour reader (CR-10, Konica Minolta Japan, Inc., Tokyo, Japan) and expressed as L*a*b* and ΔE^*_{ab} values [23]. In the former system, L* represents brightness, equalling zero for a black diffuser and 100 for a perfectly reflecting one; a* represents colour on the red-green axis, being positive for red and negative for green; b* represents colour on the blue-yellow axis, being positive for yellow and negative for blue. The colour difference was calculated as $\Delta E^*_{ab} = ((\Delta L^*)^2 + (\Delta a^*)^2 + (\Delta b^*)^2)^{1/2}$, where ΔL^* is the difference in brightness between two vivid surfaces, and Δa^* and Δb^* are the differences in the colour coordinates a* and b*, respectively. TVOC concentrations were calculated by GC-MS analysis, using a GCMS-QP2010SE (Shimadzu, Kyoto, Japan) equipped with a DB-624 fused silica capillary column (60 m × 0.25 mm i.d. × 1.4 µm film, Agilent Technologies, Santa Clara, CA, USA) and a split injection system (split ratio = 11:1). The experimental conditions employed for the GC-MS

analysis and the solid-phase extraction from the fabrics were taken from a previous publication [8]. The initial oven temperature of 35 °C was held for 15 min and then raised to 240 °C over 8 min at a rate of 6 °C/min. The adsorbed odour components were desorbed by blowing 60 L (0.5 L/min) of air, re-adsorbed onto a charcoal tube, extracted with 1 mL of carbon disulphide, and analysed by GC-MS. TVOC concentrations calculated for all compounds eluted between *n*-hexane and *n*-hexadecane were calibrated and converted to toluene equivalents.

The experimental methods and conditions employed for the detection of smoke components are summarized in Figure 10. The fabrics were placed inside an acryl sealed test box (1 m^3) and exposed to tobacco smoke generated by simultaneously burning five cigarettes (Mevius Original$^®$, tar: 8 mg; nicotine: 0.6 mg) in the box for 16 h [7]. The tar and odour components adsorbed on the fabric were analysed by the above-mentioned colour difference measurement and GC-MS after solid-phase extraction. Then, the other fabrics prepared at the same time were enclosed into a 5-L Tedlar$^®$ Gas Sampling Bag with 3 L of synthesized air and subjected to UV (eight black-light blue fluorescent lamps, FL20BLB (Toshiba Lighting & Technology Corporation, Yokosuka, Japan), 20 W each, 1.0 mWcm^{-2}@310–380 nm) or visible light (three fluorescent lamps, FL20SS (Panasonic Corporation, Osaka, Japan), 20 W each, 10,000 lx, UV was cut off completely by passing it through an acrylic sheet (N-169, Nitto Jushi Kogyo. Co., Ltd., Tokyo, Japan)) irradiation. The extraction of the above components from the fabrics and their analysis were carried out at specific time intervals to evaluate the corresponding time evolution and decomposition profiles (the fabrics analysed at each specific time were individual). For comparison, control experiments employing pristine and unmodified non-woven fabrics were carried out with the same methods and conditions.
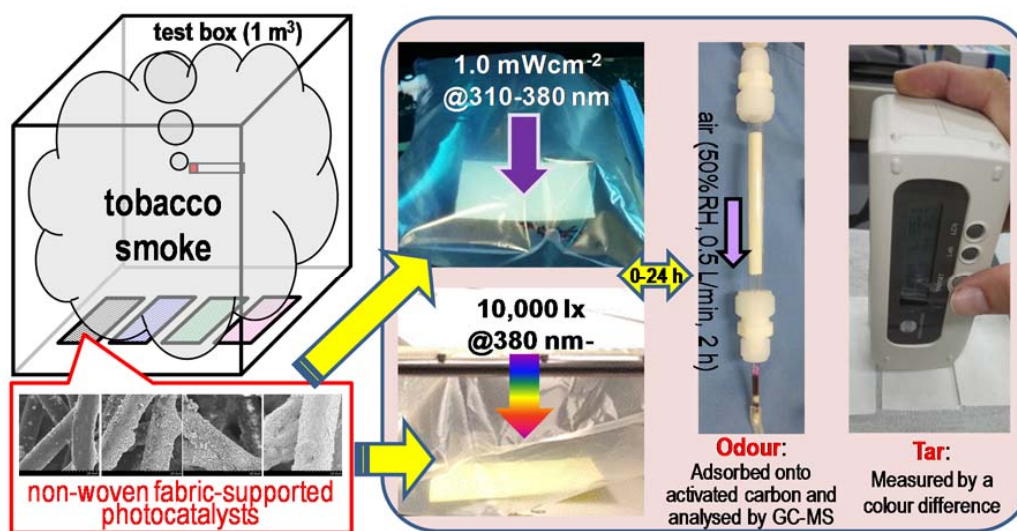

Figure 10. Schematic image of the experiments. After being exposed to tobacco smoke, the fabrics were placed under UV or visible light irradiance. Solid-phase extraction, gas chromatography-mass spectrometry (GC-MS) analysis, and the measure of the colour difference were carried out at specific time intervals, in order to evaluate the decomposition property of the odour and tar components on the catalytic system.

5. Conclusions

We described the methods employed to analyse the adsorption and decomposition of cigarette smoke pollutants by using a newly developed system—use of photocatalyst-embedded non-woven fibres. By considering three different photocatalysts, TiO$_2$, Fe(III)-grafted TiO$_2$, and Cu(II)-grafted WO$_3$, we assessed the magnitude of odour and tar constituent adsorption on the fabric fibres as well as their decomposition after specific visible light or UV irradiation periods. Among the three tested materials, the non-woven fabrics containing Fe/TiO$_2$ yielded superior results when considering the expansion of our technology for practical applications. Compared to previously reported photocatalyst systems

used for the removal of tobacco smoke components, our technique achieved higher removal ratios, as exemplified by the TVOC decomposition ratio under both UV and visible light irradiation. However, studies focusing on the fundamental understanding of the adsorption and decomposition of the odour and tar constituents of tobacco smoke trapped on clothes or other materials remain few. We believe that our study makes a significant contribution to literature because the engineering of smart materials, such as fabrics, that can intrinsically degrade cigarette smoke components is crucial in today's society, where third-hand smoke, the pollution of objects with cigarette smoke, is causing increasing numbers of health problems. We believe our proposed technology, with its simple fabrication process and effective ability, will facilitate the exploration of smart materials that can overcome the concerning effects of cigarette smoke.

Author Contributions: T.O., M.N., and Y.A. participated in the study design and conducted the study. Data were collected and analysed by T.O., D.A., and H.S. The manuscript was written by T.O. All authors have read and agreed to the published version of the manuscript.

Conflicts of Interest: The authors declare no conflict of interest.

References

1. Jacob, P.; Benowitz, N.L.; Destaillats, H.; Gundel, L.; Hang, B.; Martins-Green, M.; Matt, G.E.; Quintana, P.J.E.; Samet, J.M.; Schick, S.F.; et al. Thirdhand smoke: New evidence, challenges, and future directions. *Chem. Res. Toxicol.* **2017**, *30*, 270–294. [CrossRef]

2. Winickoff, J.P.; Friebely, J.; Tanski, S.E.; Sherrod, C.; Matt, G.E.; Hovell, M.F.; McMillen, R.C. Beliefs about the health effects of "thirdhand" smoke and home smoking bans. *Pediatrics* **2009**, *123*, e74–e79. [CrossRef]

3. Poppendieck, D.; Gong, M.; Pham, V. Influence of temperature, relative humidity, and water saturation on airborne emissions from cigarette butts. *Sci. Total Environ.* **2020**, *712*, 136422. [CrossRef] [PubMed]

4. Fujishima, A.; Honda, K. Electrochemical photolysis of water at a semiconductor electrode. *Nature* **1972**, *238*, 37–38. [CrossRef] [PubMed]

5. Ochiai, T.; Fujishima, A. Photoelectrochemical properties of TiO_2 photocatalyst and its applications for environmental purification. *J. Photochem. Photobiol. C* **2012**, *13*, 247–262. [CrossRef]

6. Slimen, H.; Ochiai, T.; Nakata, K.; Murakami, T.; Houas, A.; Morito, Y.; Fujishima, A. Photocatalytic Decomposition of cigarette smoke using a TiO_2-impregnated titanium mesh filter. *Ind. Eng. Chem. Res.* **2012**, *51*, 587–590. [CrossRef]

7. Ochiai, T.; Hayashi, Y.; Ito, M.; Nakata, K.; Murakami, T.; Morito, Y.; Fujishima, A. An effective method for a separation of smoking area by using novel photocatalysis-plasma synergistic air-cleaner. *Chem. Eng. J.* **2012**, *209*, 313–317. [CrossRef]

8. Ochiai, T.; Ichihashi, E.; Nishida, N.; Machida, T.; Uchida, Y.; Hayashi, Y.; Morito, Y.; Fujishima, A. Field performance test of an air-cleaner with photocatalysis-plasma synergistic reactors for practical and long-term use. *Molecules* **2014**, *19*, 17424–17434. [CrossRef]

9. Fang, M.J.; Tsao, C.W.; Hsu, Y.J. Semiconductor nanoheterostructures for photoconversion applications. *J. Phys. D Appl. Phys.* **2020**, *53*, 143001. [CrossRef]

10. Shi, X.; Zhang, Y.; Liu, X.; Jin, H.; Lv, H.; He, S.; Hao, H.; Li, C. A mild in-situ method to construct Fe-doped cauliflower-like rutile TiO_2 photocatalysts for degradation of organic dye in wastewater. *Catalysts* **2019**, *9*, 426. [CrossRef]

11. Yu, H.; Irie, H.; Shimodaira, Y.; Hosogi, Y.; Kuroda, Y.; Miyauchi, M.; Hashimoto, K. An efficient visible-light-sensitive Fe(III)-grafted TiO_2 photocatalyst. *J. Phys. Chem. C* **2010**, *114*, 16481–16487. [CrossRef]

12. Irie, H.; Miura, S.; Kamiya, K.; Hashimoto, K. Efficient visible light-sensitive photocatalysts: Grafting Cu(II) ions onto TiO_2 and WO_3 photocatalysts. *Chem. Phys. Lett.* **2008**, *457*, 202–205. [CrossRef]

13. Ochiai, T.; Fukuda, T.; Nakata, K.; Murakami, T.; Tryk, D.; Koide, Y.; Fujishima, A. Photocatalytic inactivation and removal of algae with TiO$_2$-coated materials. *J. Appl. Electrochem.* **2010**, *40*, 1737–1742. [CrossRef]

14. JIS A 1965. *Determination of Volatile Organic Compounds in Indoor and Test Chamber Air by Active Sampling on Tenax TA® Sorbent, Thermal Desorption and Gas Chromatography Using MS or MS-FID*; Japanese Standards Association: Tokyo, Japan, 2015.

15. Yi, X.; Zhu, Y.; Wang, D.; Yang, F.; Wang, Y.; Shi, W. Adsorption mechanism of oil-in-water on a TiO$_2$/Al$_2$O$_3$–polyvinylidene fluoride (PVDF) ultrafiltration membrane. *Langmuir* **2018**, *34*, 9907–9916. [CrossRef]

16. Shuai, Q.; Yang, X.; Luo, Y.; Tang, H.; Luo, X.; Tan, Y.; Ma, M. A superhydrophobic poly(dimethylsiloxane)-TiO$_2$ coated polyurethane sponge for selective absorption of oil from water. *Mater. Chem. Phys.* **2015**, *162*, 94–99. [CrossRef]

17. Dias Filho, N.L. Adsorption of Cu(II) and Co(II) complexes on a silica gel surface chemically modified with 2-mercaptoimidazole. *Microchim. Acta* **1999**, *130*, 233–240. [CrossRef]

18. Bamwenda, G.R.; Sayama, K.; Arakawa, H. The effect of selected reaction parameters on the photoproduction of oxygen and hydrogen from a WO$_3$-Fe^{2+}-Fe^{3+} aqueous suspension. *J. Photochem. Photobiol. A* **1999**, *122*, 175–183. [CrossRef]

19. Qiu, X.; Miyauchi, M.; Sunada, K.; Minoshima, M.; Liu, M.; Lu, Y.; Li, D.; Shimodaira, Y.; Hosogi, Y.; Kuroda, Y.; et al. Hybrid Cu$_x$O/TiO$_2$ Nanocomposites as risk-reduction materials in indoor environments. *ACS Nano* **2012**, *6*, 1609–1618. [CrossRef]

20. Chiu, Y.H.; Chang, T.F.M.; Chen, C.Y.; Sone, M.; Hsu, Y.J. Mechanistic insights into photodegradation of organic dyes using heterostructure photocatalysts. *Catalysts* **2019**, *9*, 430. [CrossRef]

21. Sakatani, Y.; Okusako, K.; Suyasu, Y.; Murata, M.; Inoue, K.; Oki, Y. Development of a highly active visible light driven photocatalyst. *Sumitomo Kagaku R D Rep.* **2009**, *1*, 14–23.

22. Cieślak, M.; Schmidt, H.; Twarowska-Schmidt, K.; Kamińska, I. Removal of nicotine from indoor air using titania-modified polypropylene fibers: Nicotine decomposition by titania-modified polypropylene fibers. *Int. J. Environ. Sci. Technol.* **2017**, *14*, 1371–1382. [CrossRef]

23. JIS 8722. *Methods of Colour Measurement-Reflecting and Transmitting Objects*; Japanese Standards Association: Tokyo, Japan, 2009.